ORIGINAL ARTICLE

Orbit and clock analysis of Compass GEO and IGSO satellites

**P. Steigenberger · U. Hugentobler · A. Hauschild ·
O. Montenbruck**

Abstract China is currently focussing on the establishment of its own global navigation satellite system called Compass or BeiDou. At present, the Compass constellation provides four usable satellites in geostationary Earth orbit (GEO) and five satellites in inclined geosynchronous orbit (IGSO). Based on a network of six Compass-capable receivers, orbit and clock parameters of these satellites were determined. The orbit consistency is on the 1–2 dm level for the IGSO satellites and on the several decimeter level for the GEO satellites. These values could be confirmed by an independent validation with satellite laser ranging. All Compass clocks show a similar performance but have a slightly lower stability compared to Galileo and the latest generation of GPS satellites. A Compass-only precise point positioning based on the products derived from the six-receiver network provides an accuracy of several centimeters compared to the GPS-only results.

Keywords GNSS · BeiDou-2 · Satellite orbits · Allan deviation

1 Introduction

Since the 1990s China is working on the development of its own satellite navigation system called Compass or Bei-Dou. BeiDou-1 was a regional system consisting of two geostationary satellites (BeiDou 1A and 1B launched in October and December 2000, respectively) and a backup

P. Steigenberger (✉) · U. Hugentobler
Institut für Astronomische und Physikalische Geodäsie,
Technische Universität München, 80290 München, Germany
e-mail: steigenberger@bv.tum.de

A. Hauschild · O. Montenbruck
German Space Operations Center, Deutsches Zentrum für
Luft- und Raumfahrt, 82230 Weßling, Germany

satellite (BeiDou 1C launched in May 2003). The BeiDou-1 services were declared operational in mid of 2003 (Qian et al. 2012) and were available for civilian users since April 2004 (Chen et al. 2009). Positioning with BeiDou-1 was based on two-way transmissions and could provide an accuracy of about 100 m (Dragon in Space 2012).

In contrast to BeiDou-1 with regional coverage and a two-way measurement principle, Compass/BeiDou-2 is ultimately conceived as a Global Navigation Satellite System (GNSS) based on one-way measurements like the US Global Positioning System (GPS), the Russian GLONASS, or the European Galileo system. The first satellite Compass M-1 was launched in April 2007 (Jun et al. 2012). Starting with 2010, the number of launches per year was significantly increased (see Table 1) resulting in currently 14 active Compass satellites. In contrast to other GNSSs, Compass consists of three different types of orbits:

- Medium Earth orbit (MEO): comparable to the GPS, GLONASS, and Galileo orbits with an altitude of about 27,900 km, an inclination of 55° and a period of revolution of $12^h\,53^m$.
- Inclined geosynchronous orbit (IGSO) with an altitude of about 35,787 km, an inclination of 55°, an eccentricity of $e < 0.003$, and a period of revolution of $23^h\,56^m$ resulting in a daily repeat groundtrack with a symmetric figure of eight, see Fig. 1.
- Geostationary Earth orbit (GEO) also with an altitude of about 35,787 km. According to their name, these satellites have an almost constant position in an Earth-fixed system. However, due to a non-zero inclination of $0.7° - 1.7°$, a certain north–south movement can be seen in Fig. 1. To compensate the east–west drift, regular maneuvers have to be performed which are discussed in detail in Sect. 3.2.

Table 1 Compass constellation status

Satellite	PRN	NORAD-ID	COSPAR-ID	Launch date	Mean longitude
G1	C01	36287	2010-001A	16 January 2010	140.0°E
G2	C02	34779	2009-018A	14 April 2009	n/a
G3	C03	36590	2010-024A	02 June 2010	84.0°E
G4	C04	37210	2010-057A	31 October 2010	159.9°E
G5	C05	38091	2012-008A	14 February 2012	58.7°E
I1	C06	36828	2010-036A	31 July 2010	120.1°E
I2	C07	37256	2010-068A	17 December 2010	117.9°E
I3	C08	37384	2011-013A	09 April 2011	119.9°E
I4	C09	37763	2011-038A	26 July 2011	94.8°E
I5	C10	37948	2011-073A	01 December 2011	94.7°E
M1	C30	31115	2007-011A	13 April 2007	–
M3	C11	38250	2012-018A	29 April 2012	–
M4	C12	38251	2012-018B	29 April 2012	–
M5	C13	38774	2012-050A	18 September 2012	–
M6	C14	38775	2012-050B	18 September 2012	–

The first character of the satellite name refers to the orbit type: *G* geostationary orbit, *I* inclined geosynchronous orbit, *M* medium Earth orbit
C02 does not transmit navigation signals and is drifting unstabilized in the equatorial plane (Flohrer et al. 2011)

Whereas MEO satellites provide global coverage, the IGSO and GEO satellites are visible within a limited area, therefore providing only regional services. By the end of 2012, phase 1 of Compass should be concluded with an emphasis on these regional navigation capabilities and a constellation of five GEO, five IGSO, and four MEO satellites (Shi et al. 2013). In phase 2, global coverage is aimed to be achieved by increasing the number of MEO satellites to 27 by 2020 (accompanied by five GEO and three IGSO satellites). The investigations discussed in this study are limited to the currently active four GEO and five IGSO satellites. The MEO satellites are not considered due to the problems of Compass M-1 described by Hauschild et al. (2012a) and the lack of global tracking data.

All Compass satellites transmit triple-frequency navigation signals as listed in Table 2. The B1 band is close to the GPS L1 frequency of 1,575.42 MHz and the B3 band close to the Galileo E6 with 1,278.52 MHz. The B2 frequency is identical with Galileo E5b. End of 2011, a draft version of the Compass Interface Control Document (ICD) was released (China Satellite Navigation Office 2011) and initial operational capability of the regional service was declared. However, the draft ICD only contains information on the B1 frequency. A tracking of the B2 and B3 signals is only possible due to knowledge about the signal structure and ranging codes obtained from analyses with a high-gain antenna (Gao et al. 2009).

A general overview of the Compass system design is given in Qian et al. (2012). First results on Compass signal analysis
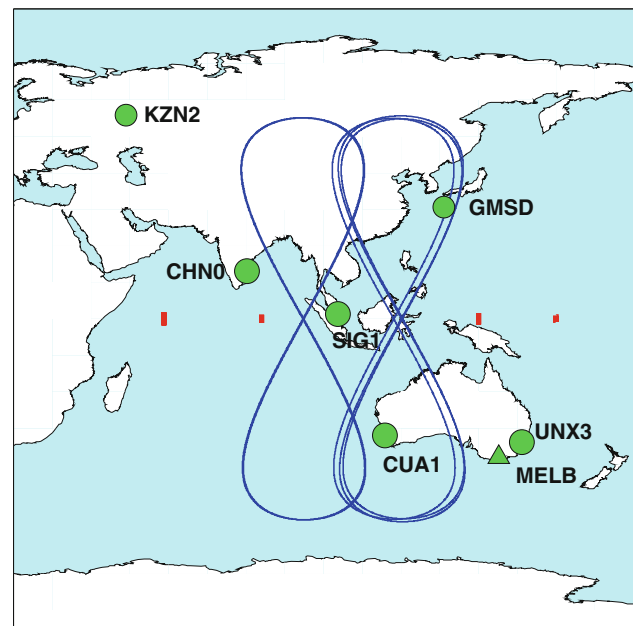
Fig. 1 Compass-capable tracking stations and ground tracks of the IGSO (*blue*) and GEO (*red*) satellites. Stations used in the orbit and clock determination are indicated by *circles*. The Melbourne station used for the positioning experiment is indicated by a *triangle*

and clock performance are discussed in Gong et al. (2012), Hauschild et al. (2012b), Jun et al. (2012), and Montenbruck et al. (2012). The Compass satellite orbits determined by Shi et al. (2012) have a radial orbit precision of 10 cm. Ge et al.

Table 2 Frequencies of the three Compass bands

Band	Freq. (MHz)	Comment
B1	1,561.098	Close to GPS L1
B2	1,207.14	Same as Galileo E5b
B3	1,268.52	Close to Galileo E6

(2012) also report radial orbit overlap RMS values of about 1 dm. However, as the RMS values in along-track direction are much larger, Ge et al. (2012) give 3D overlaps of 3.3 m for the GEO and 0.5 m for the IGSO satellites. Based on broadcast orbits and clocks, Gao et al. (2012) achieved a positioning accuracy of 20 m for the horizontal and 30 m for the vertical component. Using precise orbit products for a relative positioning on a baseline of a few hundred meters, Shi et al. (2013, 2012) reached accuracies of 1–4 cm for a kinematic solution. Static precise point positioning (PPP) resulted in RMS differences of 2–5 cm w.r.t. GPS-only solutions; similar accuracies are also reported by Ge et al. (2012). Montenbruck et al. (2012) even achieved a sub-centimeter accuracy on a very short baseline of 8 m by resolving extra-wide-lane ambiguities based on triple-frequency observations.

This publication aims at the determination of precise Compass orbit and clock products as well as their application for positioning. It is based on the experiences obtained from the orbit and clock determination of the Galileo test satellite GIOVE-B (Steigenberger et al. 2011) and QZS-1, the first satellite of the Japanese Quasi-Zenith Satellite System (QZSS, Steigenberger et al. 2012). However, several modifications in the processing were necessary due to different frequencies and in particular due to different characteristics of the GEO orbits (attitude mode, orbit parameterization, maneuver detection and handling). All Compass-related studies of Chinese authors listed before are based on tracking data of national GNSS equipment and possibly non-public information about the Compass system (e.g., antenna offsets and attitude behavior). In contrast to that, our studies are based on independently developed GNSS hardware with well-characterized tracking performance for legacy navigation systems. Furthermore, the processing is strictly based on publicly available information and can thus provide an independent evaluation of the Chinese results.

Section 2 introduces the GNSS tracking network and the processing strategy for orbit and clock determination. The code biases originating from using different GNSS, different frequencies, different receivers, and even different firmware versions are discussed. In contrast to Montenbruck et al. (2012) who only used 1-day orbits, multi-day arcs are computed to achieve a better orbit accuracy. The impact of different sets of orbit parameters as well as orbital arc lengths on the orbit precision is evaluated in Sect. 3 and the maneuvers of the GEO satellites are analyzed. Section 4

demonstrates the Compass clock performance. Finally, the Compass orbit and clock products are utilized for a Compass-only PPP whose results are compared with GPS-only solutions in Sect. 5.

2 GNSS processing

The orbit and clock analysis presented in this paper is based on up to six stations listed in Table 3 and shown in Fig. 1. The stations in Singapore and Sydney are part of the Cooperative Network for GIOVE observation (CONGO, Montenbruck et al. 2010). Data from the Kazan and Nakatane stations are provided via the Multi-GNSS Experiment (M-GEX) of the International GNSS Service (IGS, Dow et al. 2009; Weber 2012). Data from Chennai are provided by Trimble, the Curtin station is operated by Curtin University. The orbit and clock results discussed in this paper are based on these six stations for the time period 19 March until 7 May 2012 (day of year 79–128/2012). Data from the Melbourne station were provided for five complete days by Trimble through Curtin University and were used for Compass-only PPP discussed in Sect. 5.

Two different types of receivers are employed at the seven stations. Whereas the Trimble NetR9 is capable of tracking all three Compass frequencies, the Septentrio AsteRx3 only provides B1 and B2 observations. Therefore, the analysis in this paper is limited to these two frequencies. The various antenna types employed at the stations are all designed for multi-GNSS use and cover the full set of Compass and GPS frequency bands.

2.1 Processing strategy

In general, there are two different approaches to determine Compass orbit and clock parameters: (1) all parameters are estimated from Compass observations only; (2) GPS observations are used in addition to derive parameters common to both GNSS (in particular station coordinates, but also receiver clock and troposphere parameters). The latter approach benefits from the fully employed GPS constellation and results in a better quality of the estimated parameters. Therefore, we use this approach and process dual-frequency GPS and Compass data with a modified version of the Bernese GPS Software (Dach et al. 2007; Svehla et al. 2008). A first step is based on a GPS-only PPP utilizing the rapid products of the Center for Orbit Determination in Europe (CODE, Dach et al. 2009) followed by a Compass-only step as discussed for the Galileo test satellite GIOVE-B in Steigenberger et al. (2011). GPS and Compass data in RINEX 3 (Gurtner and Estey 2009) format are processed with a sampling rate of 30 s. Station coordinates, troposphere zenith delays and gradients as well as receiver clock

Table 3 Compass-capable tracking stations

Abb.	Location	Country	Receiver	Antenna	Radome
CHN0	Chennai	India	TRIMBLE NETR9	TRM55971.00	NONE
CUA1	Curtin	Australia	TRIMBLE NETR9	TRM59800.00	SCIS
GMSD	Nakatane	Japan	TRIMBLE NETR9	TRM59800.00	SCIS
KZN2	Kazan	Russia	TRIMBLE NETR9	TRM59800.00	SCIS
MELB	Melbourne	Australia	TRIMBLE NETR9	TRM55971.00	SCIS
SIG1	Singapore	Rep. of Singapore	TRIMBLE NETR9	LEIAR25.R3	LEIT
UNX3	Sydney	Australia	SEPT ASTERX3	LEIAR25.R3	LEIT

Table 4 Important options of the GNSS processing

Basic observable GPS	L1 and L2 code and carrier phase observations
Basic observable Compass	B1 and B2 code and carrier phase observations
Modeled observable	Ionosphere-free linear combination
Observation weighting	Elevation-dependent weighting with $\frac{1}{\cos^2 z}$
	Relative weighting of code and phase observations: 1:100
Sampling rate	30 s
Elevation cutoff angle	5°
Tidal displacements	IERS Conventions 2003 (McCarthy and Petit 2004), FES2004 (Lyard et al. 2006)
Troposphere modeling	NMF (Niell 1996), hydrostatic a priori delays according to Dach et al. (2007)
Phase polarization	Wu et al. (1993)
Relativistic effects	IERS Conventions 2003 (McCarthy and Petit 2004)

parameters are estimated from GPS code and phase observations. These parameters are kept fixed when solving for the Compass-related parameters: Six Keplerian elements, one to nine radiation pressure (RPR) parameters (see Sec. 3.1) of the model of Beutler et al. (1994), epoch-wise satellite clock corrections, and differential code biases (DCBs).

For Compass, ionosphere-free linear combinations of B1 and B2 code and phase observations are used. To account for systematic differences of the Compass code observables w.r.t. the GPS L1 and L2 code data, DCBs are estimated. The bias of the Sydney station is fixed to zero as a reference since the biases cannot be determined in an absolute sense. As a description of the broadcast message is not available, Compass a priori orbits are taken from Two Line Elements (TLEs) provided by https://www.space-track.org. However, the orbit quality of these a priori orbits is fairly limited (differences of several tens of km to the estimated orbit). Therefore, three orbit iterations have to be done to ensure a converged solution.

Due to the limited public information about the Compass spacecraft design, several assumptions have to be made:

– For the IGSO satellites, yaw attitude as for the GPS satellites (Bar-Sever 1996) is assumed.
– For the GEO satellites, it is assumed that the solar panels are oriented to the Sun and normal to the orbital plane (in accord with common practice of geostationary telecommunication satellites, Soop 1994).
– Satellite vertical antenna offsets are assumed to be 1.093 m, i.e., the z-offset of the SLR retroreflector for GEO (Weiguang 2011a) as well as IGSO (Weiguang 2011b) satellites.
– Horizontal satellite antenna phase center offsets as well as the phase center variations are assumed to be zero even though some images of the Compass satellites suggest offsets at the level of several decimeters.

Receiver antenna calibrations from an anechoic chamber for GPS L1 and L2 and all Galileo bands were provided by Becker et al. (2010) for the LEIAR25.R3 and TRM55971.00 antennas. The GPS L1 and Galileo E5b calibrations were used for the Compass B1 and B2 bands. For the TRM59800.00 antennas, the GPS L1 and L2 calibrations were used. The igs08.atx antenna calibrations (Rebischung et al. 2012) were used for the GPS satellites. For further processing options, see Table 4.

2.2 Code biases

Receiver-specific differential code biases (DCBs) are estimated to account for systematic differences between

Table 5 Differential code biases with respect to the reference receiver in Sydney (Septentrio AsteRx3)

Station	Receiver/Firmw.	DCB (ns)	STD (ns)
CHN0	NetR9 FW 4.60	31.9	0.35
CUA1	NetR9 FW 4.4x	1,931.1	0.73
GMSD	NetR9 FW 4.4x	1,943.9	0.48
KZN2[a]	NetR9 FW 4.4x	1,571.8	0.77
KZN2[b]	NetR9 FW 4.4x	1,939.7	0.43
SIG1	NetR9 FW 4.4x	1,938.1	0.34

Mean values for the time period 79–125/2012 and corresponding standard deviations (STD) are given. Due to a significant discontinuity, the KZN2 time series is splitted into two time intervals. DCB estimates of NetR9 receivers with FW 4.4x include an offset of about 2 μs related to a firmware problem (see text)

[a] 79–95/2012
[b] 96–125/2012

Table 6 Station-specific mean values of the post-fit code and phase residuals (ionosphere-free linear combination) of Compass GEO and IGSO satellites

Station	Code (m)		Phase (cm)	
	IGSO	GEO	IGSO	GEO
CHN0	1.30	1.16	2.7	2.8
CUA1	1.29	1.32	1.7	2.9
GMD1	1.06	1.19	1.6	14.1
KZN2	0.81	1.51	2.0	3.1
SIG1	1.08	0.89	1.5	1.6
UNX3	1.45	1.24	1.8	1.9

30–50 ns level for different receiver types with a mean STD of 0.7 ns (Hauschild and Steigenberger 2012).
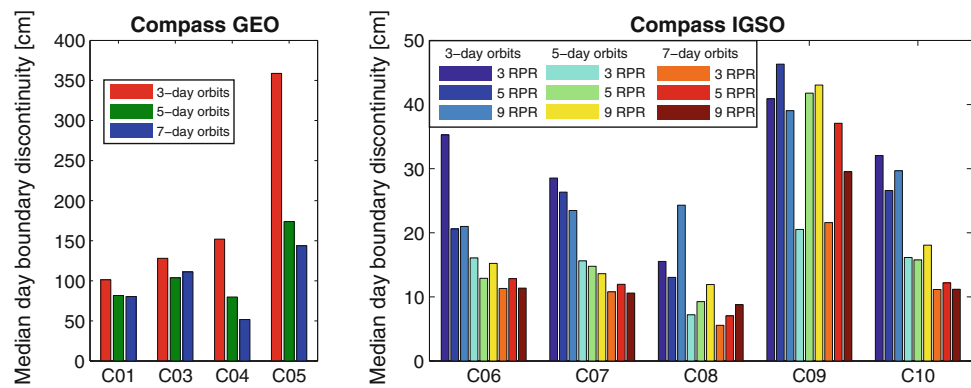
2.3 Post-fit residuals

The mean post-fit residuals of ionosphere-free code and phase observations obtained from the Compass parameter estimation are listed in Table 6. The code residuals are on the 0.9–1.5 m level and range from 0.64 to 2.23 m for individual satellites (not shown here). The largest code residuals occur at the GMSD station for C05 due to an elevation of only 6.8°. However, one has to remember that observations with low elevations are down-weighted in the parameter estimation (see Sec. 2.1). Montenbruck et al. (2012) report single-frequency pseudorange errors (including multipath) between 20 and 40 cm for mid and high elevations and up to 1 m for low elevations. Keeping in mind that these errors are amplified by a factor of about 3 when forming the ionosphere-free linear combination, the code residuals listed in Table 6 are only slightly worse.

The phase residuals in Table 6 are in general on the several centimeter level with a range of 1–53 cm for individual satellites (C05 at GMSD again has the largest residuals). All phase residuals are larger for the GEO satellites compared to the IGSO satellites. However, the differences are only 1 mm for half of the stations. For the other stations, the increased GEO residuals can be explained by one particular satellite at low elevation. Montenbruck et al. (2012) give single-frequency phase noise and multipath errors of 1–3 mm. When excluding the GEO phase residuals of GMSD, the phase residuals listed in Table 6 are larger by a factor of 3–5 reflecting the unmodeled or not properly modeled effects mentioned in Sect. 2.1.

The code residuals are in general on the same level as the residuals of GIOVE-B reported by Steigenberger et al. (2011), whereas the phase residuals are in general larger by a factor of about 1.5. However, one has to be aware that different receiver types were used and that it is in general difficult to directly draw conclusions from the residuals about the orbit accuracy.

various receiver types as well as inter-system and inter-frequency biases between GPS and Compass. These biases are composed of GNSS- and frequency-dependent delays in the satellite and receiver electronics. Different firmware (FW) versions can significantly influence these delays. For the NetR9 receivers, several different firmware versions were used in the time interval considered. Versions 4.43, 4.46, and 4.48 do not result in different bias estimates. Therefore, they are summarized as version 4.4x in the following.

The code bias of the Sydney station (Septentrio AsteRx3) is fixed to zero. Mean DCBs and corresponding standard deviations for the time interval 19 March until 4 May 2012 are listed in Table 5. The NetR9 receivers with FW 4.4x show an offset of almost 2 μs w.r.t. the reference receiver, whereas the bias of the Chennai receiver with FW 4.6 is only 32 ns. According to Riley (2012), the 2 μs bias is caused by the 4.4x firmware of the NetR9 receivers and has been fixed in later firmware releases. The firmware update to version 4.6x results in a bias consistency of the different NetR9 receivers on the level of about 10 ns. For the NetR9 at Kazan, two time intervals with significantly different DCB could be identified. The reason for this behavior is unknown, the day of the DCB discontinuity does not coincide with any equipment changes or firmware updates. The standard deviation of the daily DCB estimates is well below 1 ns for all stations.

For comparison, the DCBs of the Japanese Quasi-Zenith Satellite System (QZSS) discussed in Steigenberger et al. (2012) amount to just a few nanoseconds and are thus smaller than the Compass DCBs. With an average STD below 0.5 ns, they are also more stable than the Compass DCBs. However, one has to keep in mind that QZSS and GPS both use the same L1 and L2 signal frequencies. GPS/Galileo DCBs are on the level of ±5 ns for the same receiver type and on the

3 Orbit results

3.1 Orbit parameterization

In addition to the six Keplerian elements, dynamic parameters accounting for the radiation pressure (RPR) of the Sun have to be estimated in the orbit determination process. The model of Beutler et al. (1994) comprises a total of nine constant and periodic terms in the three axes of a Sun-oriented coordinate system. Within this paper, the following subsets of RPR parameters are considered for estimation in the orbit determination process:

– 1 parameter: direct RPR term
– 3 parameters: three constant terms only
– 5 parameters: three constant terms and one pair of sine/cosine terms in the direction perpendicular to the direction of the Sun and the solar panel axis
– 9 parameters: full set

In general, a small parameter set results in a more robust orbit determination, whereas a larger parameter set may provide an improved modeling of the actual orbit dynamics. To stabilize the orbit parameter estimates determined from a very small network of six stations only, the orbit parameters of consecutive days are combined to multi-day solutions. In the following, orbital arc lengths of 3, 5, and 7 days are used. That means, only one set of Keplerian elements and RPR parameters is estimated per arc (except for maneuvers, see Sect. 3.2).

As a quality indicator for the internal consistency of the orbits, *day boundary discontinuities* of two consecutive days are used, i.e., the 3D difference of the orbit positions at midnight between two consecutive days. Another quantity for the orbit quality is the *2-day orbit fit RMS*: a new orbit is fitted through the orbit positions of two consecutive days. The RMS of the new orbit w.r.t. the original orbit is a measure for the consistency of the original orbits (see Steigenberger et al. (2011) for a more detailed description). Finally, satellite laser

ranging (SLR) residuals provide an independent validation of the microwave-derived orbits (e.g., Urschl et al. 2005). From the multi-day solutions, only the middle day of the arc is used for the computation of the day boundary discontinuities, the orbit fit RMS values, and the SLR residuals.

First tests with these parameterizations resulted in a very bad orbit quality of the GEO satellites, in particular in the along-track direction. Depending on their location and outages of individual stations, the GEO satellites are observed by 2–6 stations simultaneously. More important, the changes of the observation geometry of the GEO satellites are much smaller compared to the IGSO satellites: as a consequence, strong correlations occur between the orbital elements, radiation pressure parameters, ambiguities, and DCBs. In particular, it is no longer possible to estimate a constant Y-bias in the solar radiation pressure model due to a pronounced correlation with the location of the orbital plane relative to the geocenter.

As a consequence of these correlations, large differences of more than 10 m occur at the day boundaries even if only three RPR parameters are estimated and multi-day arcs are used. To cope with these correlations, only one RPR parameter in the direction of the Sun is estimated for the GEO satellites. This reduction of estimated parameters significantly improves the orbit quality of the GEO satellites, although it is still worse compared to the IGSO satellites.

Day boundary discontinuities for solutions with different arc length (GEO and IGSO satellites) and different number of estimated RPR parameters (IGSO satellites only) are shown in Fig. 2. The orbit quality of the IGSO satellites is on the 1–4 dm level whereas it is worse by a factor of up to 5–7 for the GEO satellites resulting in day boundary discontinuities on the 1 m level. The quality of the GEO satellite C05 is even worse as it is only tracked by three stations resulting in a fairly limited orbit quality. The benefit of increasing the arc length is in particular pronounced for C05: the day boundary discontinuities decrease by a factor of 2 when extending the arc length from 3 to 5 days. A further extension to 7 days results in a much smaller improvement of only 17 %.

Table 7 2-Day orbit fit RMS values of Compass GEO satellites in centimeters

Arc length	RPR	C01	C03	C04	C05
3-day	1	23.2	23.2	23.3	65.6
5-day	1	22.1	22.9	18.7	37.0
7-day	1	21.6	23.2	18.1	34.7

Table 8 2-Day orbit fit RMS values of Compass IGSO satellites in centimeters

Arc length	RPR	C06	C07	C08	C09	C10
3-day	3	3.7	3.1	1.8	4.9	3.4
	5	3.0	3.0	1.8	8.1	3.2
	9	3.8	4.8	5.2	7.4	5.4
5-day	3	1.7	1.6	0.8	3.8	1.7
	5	1.8	1.9	1.3	6.5	2.0
	9	3.0	2.5	2.2	8.6	3.1
7-day	3	1.3	1.0	0.7	2.7	1.0
	5	1.7	1.6	0.9	5.1	1.5
	9	2.2	1.8	1.3	5.9	1.9

Table 9 SLR validation of the GEO satellite C01 and the IGSO satellite C08 (5-day solution with 5 RPR parameters)

Satellite	# NPT	Offset (cm)	STD (cm)	RMS (cm)
C01	10	−13.1	7.1	14.7
C08	35	21.8	9.7	23.9

In general, the orbit quality improves with increasing arc length. For most IGSO satellites, a 7-day arc with three RPR parameters provides the best performance (except for C07). Independent from the solution, C09 shows the worst day boundary discontinuities of the IGSO satellites. The IGSO orbit quality of the best solutions is on the 1–2 dm level which is similar to results for QZSS reported in Steigenberger et al. (2012) based on a regional tracking network with five stations.

The 2-day orbit fit RMS values are listed in Table 7 for the GEO and in Table 8 for the IGSO satellites. They are in general on the 2 dm level for the GEO satellites with only small changes due to different arc length. However, C05 (that already showed a bad performance in the day boundary discontinuities) is worse by a factor of 3 for the 3-day solutions but only a factor of 2 for the 5- and 7-day solutions. Compared to Fig. 2, the orbit fit RMS values are smaller by a factor of about 5 than the day boundary discontinuities. This result is expected as the day boundary discontinuities represent the differences between two individual orbit positions at one epoch, whereas the orbit fits are some kind of average over 2 days. Although the orbit fit RMS values are by far too optimistic due to the smoothing effect of multi-day solutions (the longer the arc length, the larger the smoothing effect), they allow for a relative assessment of solutions with the same arc length but different number of RPR parameters (IGSO satellites only).

The orbit fits of the IGSO satellites in Table 8 are all below 1 dm and even below 1 cm for the best performing satellites/solutions. Independent from the solution, C09 shows the worst performance of the IGSO satellites (factor 1.9– 5.7 worse than the best performing IGSO satellite per solution) as for the day boundary discontinuities. The reason for this behavior is unknown. In contrast to the orbit quality, the clock quality of C09 is the best of the IGSO satellites, see Sect. 4. For the 3-day solutions, three or five RPR parameters give the best RMS values. For the 5- and 7-day solutions, three RPR parameters give the smallest RMS values. Nine RPR parameters in general result in the worst RMS values for a fixed arc length.

Independent from the arc length, the 2-day orbit fits of the GEO satellites show a clear time dependency: the RMS values get larger with increasing elevation of the Sun above the orbital plane (close to zero at the beginning of the time interval, about 16° at the end). This effect is probably related to problems with the orbit modeling: estimating only one direct RPR parameter might be a too simple model and/or the attitude assumption of Sect. 2.1 could be erroneous. However, no information about the true attitude behavior is available. A similar behavior is visible in the time series of day boundary discontinuities but less pronounced. The IGSO satellites do not show such a time dependency.

Whereas day boundary discontinuities and orbit fit RMS values only allow evaluating the precision of the satellite orbits, SLR residuals provide the opportunity to assess the orbit accuracy as they are based on an independent observation technique. SLR retroreflector offsets for the GEO and IGSO satellites are given in Weiguang (2011a) and Weiguang (2011b), respectively. Although all Compass satellites are equipped with laser retroreflectors, only three of the GEO and IGSO satellites are presently tracked by the stations of the International Laser Ranging Service (Pearlman et al. 2002). For the time period considered in this paper, only a very limited number of normal points (NPTs) of the GEO satellite C01 and the IGSO satellite C08 are available (SLR tracking of C10 started only in July 2012): two SLR stations tracked C01 (Changchun, Yarragadee: 10 NPTs) and three SLR stations tracked C08 (Changchun, Shanghai, Yarragadee: 42 NPTs). One C08 pass of Changchun (7 NPTs) had to be excluded from the SLR analysis due to unreasonable NPT-to-NPT variations of up to 1.7 m.

Offset, standard deviation, and RMS of the SLR residuals are listed in Table 9. With STDs below 1 dm and offsets on the 1–2 dm level, these validation results are even better

Table 10 Maneuvers of Compass GEO satellites

Date	Time	Sat.	Velocity change (mm/s)				Drift accel. (mdeg/day^2)	Maneuver rate (mm/s/month)
			Total	Radial	Along-track	Cross-track		
6 Apr 2012	4:43	C01	84.3	3.5	−84.1	−5.3	−1.37	116
2 May 2012	11:00	C01	103.6	−2.1	−103.3	−7.7		
16 Apr 2012	9:11	C03	77.1	−7.1	−76.6	−4.8	−0.62	53
23 Apr 2012	7:32	C04	31.6	−2.3	−31.1	−5.3	−0.14	12
10 Apr 2012	∼1:00	C05	n/a				1.07	−91

The exact time and the velocity change of the maneuver of C05 could not be determined properly due to only 2–3 stations tracking this satellite. Following the estimated Δv, the drift acceleration due to asphericity of the Earth is provided for the respective sub-satellite longitude of each GEO. The last column lists the maneuver magnitude needed to compensate for the drift acceleration

compared to the day boundary discontinuities, in particular for the GEO satellite C01. However, one has to keep in mind that the SLR validation primarily assesses the radial component, whereas the largest errors occur in the along-track direction.

3.2 GEO orbit maneuvers

Compass is the only GNSS with geostationary satellites being a part of the nominal satellite constellation. Due to gravitational perturbations of Earth, Sun, and Moon, station-keeping maneuvers are necessary in regular intervals to maintain the designated positions in the equatorial plane (Soop 1994). According to Jun et al. (2012), east–west (or longitude) station-keeping maneuvers are performed every 25 to 35 days and north–south (or inclination) maneuvers every 2 years. The maneuvers of the Compass GEO satellites detected from the orbit analysis of the 50-day test period are listed in Table 10. All maneuvers are east–west maneuvers. The main velocity change occurs in the along-track direction with velocity changes of up to 100 mm/s. The negative sign stands for decelerating the satellite and thus lowering the orbital height.

In the case of a maneuver, separate sub-arcs are set up for the maneuvering satellite in a multi-day solution, i.e., separate orbital elements and radiation pressure parameters before and after the maneuver are estimated. For an ideal maneuver modeling, the two independent orbital arcs would intersect in one point. However, due to errors in the orbit determination, the two orbits in general do not intersect. Therefore, the maneuver time as well as the velocity changes listed in Table 10 are determined from the closest approach of these two separate arcs.

C01 is the only satellite with two maneuvers separated by 26 days, for each of the other GEO satellites only a single maneuver takes place. However, as only a 50-day time interval is considered in the analysis, the maneuver frequency is well within the general operations concept given by Jun et al. (2012). The sub-satellite longitude of individual GEOs

varies by ±0.1° to ±0.15° and the latitude by ±0.8° to ±1.8°. Compared to other GEO satellites, this control box is large: typical values are ±0.1° in east–west and north–south direction (Withers 1999).

The drift accelerations given in Table 10 were derived from Montenbruck (2009) based on the mean longitude given in Table 1. The drift acceleration of C04 is small compared to the other GEO satellites as it is located close to an unstable point at 162°E, where the acceleration is almost zero. The last column of Table 10 lists the velocity changes necessary to compensate for the drift acceleration accumulated during 1 month. Assuming a common control window size for all Compass GEOs would require a maneuver spacing of 22–79 days, i.e., a wider range than the 25–35 days given in Jun et al. (2012).

4 Clock results

All Compass satellites are equipped with Rubidium clocks from manufacturers in Switzerland and China (Han et al. 2011). To assess the performance of the Compass on board clocks, modified Allan deviations computed from the 30 s clock estimates are shown in Fig. 3. Median values per satellite were derived from all days with complete clock estimates (i.e., no data gaps). In general, the clock performance of the IGSO and GEO satellites is on the same level. The bad orbit performance of C05 mentioned in Sect. 3 reflects itself in an increased modified Allan deviation of the apparent clock at longer integration times which is most likely unrelated to the physical clock behavior. Compared to the Rubidium clock of the first Galileo in-orbit validation satellite (IOV-1), the apparent performance of the Compass clocks is in general worse by a factor of about 2, in particular at longer integration times. However, at shorter periods, the C03 clock seems to be competitive with the IOV-1 clock although both do not reach the stability level of the latest generation of GPS Rubidium clocks (G25 shown as an example for the GPS IIF satellites).

Fig. 3 Modified Allan deviation of Compass GEO (*left*) and IGSO (*right*) satellites. Median values for the time period 79–128/2012 are shown. For comparison purposes, the performance of the first Galileo IOV satellite (E11) and the first GPS block IIF satellite (G25) Rubidium clocks are also shown in the *left plot*
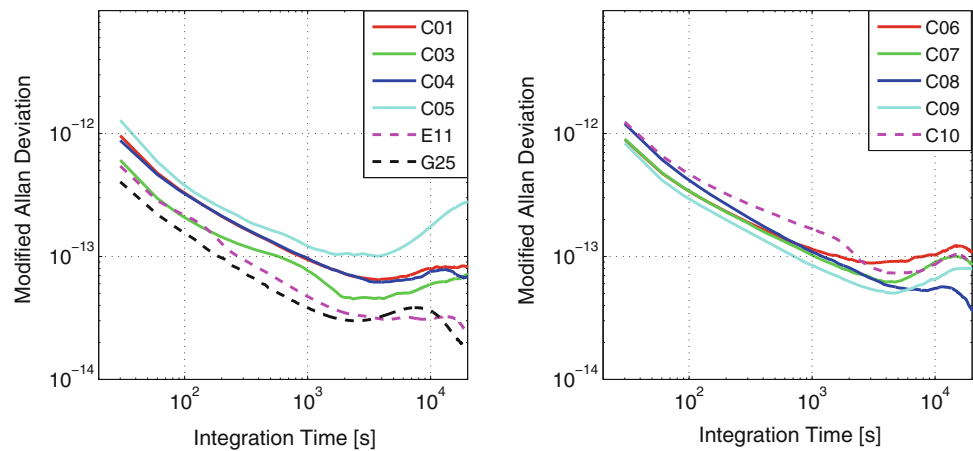
At an integration time of 1,000 s, the GEO satellites show an Allan deviation between 8 and 12×10^{-14}; the performance of the IGSO clocks is similar with values between 8 and 17×10^{-14}. These results are in general slightly better than those of Montenbruck et al. (2012) based on a three-way carrier phase approach (Hauschild et al. 2012b). The degraded clock performance of C10 compared to the other IGSO satellites already mentioned by Montenbruck et al. (2012) is also evident in Fig. 3.

The Allan deviation of the best performing IGSO satellite C09 given in Gong et al. (2012) is also slightly worse compared to the present study. Gong et al. (2012) show Allan deviations of 40×10^{-14} at an integration time of 100 s and 10×10^{-14} at 1,000 s with smoothed broadcast ephemeris compared to 30×10^{-14} and 8×10^{-14} in the present study (see Fig. 3). This effect might have two different explanations: (1) degraded orbit quality of the smoothed broadcast orbits compared to our post-processed multi-day orbits; (2) quality of the reference clock. The reference clock for the clock solutions shown in Fig. 3 is a highly stable hydrogen maser used in the CODE solution as reference, whereas the reference clock is not explicitly specified in Gong et al. (2012).

Median values of the clock drift are given in Table 11. For C05, two different time intervals are given due to a changed clock behavior, probably due to a clock adjustment. Except for the first time period of C05, all clock drifts are in the range of 0.7–7 µs/day. These values are in good agreement with Montenbruck et al. (2012) and in the same order of magnitude as the GPS satellite clocks.

5 Compass-only PPP

For 5 days (28 March–1 April 2012), data of an additional tracking station in Melbourne (MELB, Australia) were provided by Trimble and Curtin University (Perth, Australia) to test the PPP performance of the orbit and clock products

Table 11 Median values of Compass clock drift

Satellite	PRN	No. of days	Drift (µs/day)
G1	C01	38	3.56
G3	C03	29	0.67
G4	C04	37	−0.66
G5	C05	15[a]	−27.39
		17[b]	1.23
I1	C06	41	1.37
I2	C07	42	0.67
I3	C08	46	1.34
I4	C09	44	−6.47
I5	C10	48	−2.08

Only full days without gaps are considered
[a] 79–106/2012
[b] 107–128/2012

Table 12 Results of Compass-only PPP: RMS differences of five daily solutions w.r.t. GPS-only station coordinates

Satellites	North (cm)	East (cm)	Up (cm)
IGSO + GEO	1.7	4.1	6.4
IGSO	2.0	5.1	11.7

discussed above. The Compass visibility is quite limited at Melbourne with 5–8 satellites simultaneously visible mainly in the north–west quadrant. As a consequence, the GDOP varies between 3.6 and 8.2. In addition to the station coordinates, troposphere zenith delays with 2 h parameter spacing, epoch-wise receiver clocks, and float ambiguities were estimated.

The RMS differences between GPS-only and Compass-only coordinate estimates shown in Table 12 are on the several centimeter level. Although the GEOs have a worse orbit accuracy compared to the IGSOs, they significantly improve the Compass-only positioning accuracy, in particular for the height component. The accuracy of the Compass-only PPP
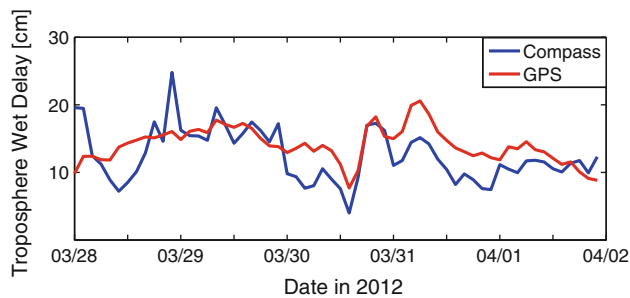
Fig. 4 GPS-only and Compass-only troposphere wet delays of station Melbourne (2 h parameter spacing)

is in the same order of magnitude as the results of Shi et al. (2012). They used a larger ground network of 15 stations but only four IGSO and three GEO satellites for the generation of satellite orbits and clocks used for their PPP experiment also covering a period of 5 days. The RMS differences in Table 12 are slightly better than results given in Montenbruck et al. (2012) based on 4 days of the same receiver at Melbourne. The reason for this improvement is the better accuracy of orbits and clocks based on multi-day solutions compared to the 1-day products used by Montenbruck et al. (2012).

The PPP performance of the orbits and clocks computed with different arc length and number of RPR parameters is on a similar level: the RMS differences w.r.t. the GPS-only solution range from 1.4 to 2.7 cm for the north component, 2.8 to 4.9 cm for the east component and 5.2 to 7.1 cm for the height component. No clearly superior solution could be identified.

The troposphere zenith wet delays (ZWDs) derived from GPS and Compass (Fig. 4) in general show a similar behavior. However, due to the smaller and more variable satellite number, the Compass ZWDs are much more noisy. This is not astonishing due to the smaller observation number and reduced coverage of the sky for Compass compared to GPS. The GPS/Compass ZWD differences show a bias of 1.5 cm and have a standard deviation of 3.4 cm.

Systematic biases of the GPS and Compass become manifest in the receiver clock estimates. The mean bias (DoY 89 excluded due to an outage-induced clock jump) between the GPS-only and Compass-only receiver clock parameters is with 1,953.7 ns in the same order of magnitude as the DCBs of the NetR9 receivers with firmware 4.4x used in the orbit and clock determination (see Table 5).

6 Conclusions

Compass orbit and clock parameters were estimated with a small tracking network of four to six stations. An orbit accuracy on the several decimeter level for the GEO and few decimeter level for the IGSO satellites could be achieved.

Due to the limited knowledge of the Compass system, several assumptions had to be made that might be erroneous. More detailed knowledge of the satellite behavior will contribute to an improved modeling of the satellites and as a consequence to a better orbit quality. In particular, information on Compass attitude modes and antenna offsets will be required to fully exploit the accuracy of the available observations. However, the biggest problems of the GEO orbit determination are the small changes in the observation geometry responsible for large correlations between the estimated parameters. Limiting the number of RPR parameters to only one direct parameter helped to cope with these correlations, but the dependence of the orbit quality on the position of the Sun above the orbital plane also shows the deficits of this approach. On the other hand, the large orbit errors encountered in the GEO orbit determination do not render them useless for positioning, since the large along-track errors have only a 5–10 % contribution to the modeled pseudorange on average.

Code biases due to different satellite systems and frequencies are on the level of up to 10 ns for the same receiver type but can reach up to 30 ns, if different receivers are used. The stability of the Compass GEO and IGSO clocks is on a similar level, although it is slightly worse compared to other GNSS. Precise orbit and clock products for the regional Compass system allow for a precise point positioning with Compass observations only. Although the Compass visibility conditions for the Compass-only PPP were not optimal, a few centimeter accuracy compared to GPS could be achieved.

A larger tracking network, in particular a network providing global coverage for the MEO satellites is an important step for the further improvement of the Compass orbit and clock products. However, this is probably only a matter of time, as more and more Compass-capable receivers are employed, in particular in the framework of the IGS M-GEX project. A major deficiency of Compass (in particular for real-time users) is the lack of public availability of broadcast orbits as the corresponding information is not published in the preliminary version of the ICD. The situation will hopefully change in the near future with the publication of the full ICD.

References

Bar-Sever Y (1996) A new model for GPS yaw attitude. J Geod 70(1):714–723. doi:10.1007/BF00867149

Becker M, Zeimetz P, Schönemann E (2010) Antenna chamber calibrations and antenna phase center variations for new and existing GNSS signals. In: IGS workshop 2010, 28 June–2 July 2010, Newcastle

Beutler G, Brockmann E, Gurtner W, Hugentobler U, Mervart L, Rothacher M, Verdun A (1994) Extended orbit modeling techniques at the CODE processing center of the international GPS service for geodynamics (IGS): theory and initial results. Man Geod 19:367–386

Chen H, Huang Y, Chiang K, Yang M, Rau R (2009) The performance comparison between GPS and BeiDou-2/COMPASS: a perspective from Asia. J Chin Inst Eng 32(5):679–689

China Satellite Navigation Office (2011) BeiDou Navigation Satellite System signal. In: Space interface control document (test version). Technical report. http://www.beidou.gov.cn/attach/2011/12/27/201112273f3be6124f7d4c7bac428a36cc1d1363.pdf

Dach R, Hugentobler U, Fridez P, Meindl M (eds) (2007) Bernese GPS Software Version 5.0. Astronomical Institute, University of Bern, Bern

Dach R, Brockmann E, Schaer S, Beutler G, Meindl M, Prange L, Bock H, Jäggi A, Ostini L (2009) GNSS processing at CODE: status report. J Geod 83(3–4):353–365. doi:10.1007/s00190-008-0281-2

Dow J, Neilan R, Rizos C (2009) The International GNSS Service in a changing landscape of Global Navigation Satellite Systems. J Geod 83(3–4):191–198. doi:10.1007/s00190-008-0300-3

Dragon in Space (2012). http://www.dragoninspace.com/navigation/beidou.aspx. Accessed 04–09–2012

Flohrer T, Choc R, Bastida B (2011) Classification of geosynchronous objects. Issue 13. European Space Agency, Space Debris Office, GEN-DB-LOG-00074-OPS-GR

Gao GX, Chen A, Lo S, Lorenzo DD, Walter T, Enge P (2009) Compass-M1 broadcast codes in E2, E5b, and E6 frequency bands. IEEE J Sel Top Signal Process 3(4):599–612. doi:10.1109/JSTSP.2009.2025635

Gao Z, Zhang H, Hu Z, Peng J (2012) Performance analysis of BeiDou Satellite Navigation System (4IGSO + 3GEO) in standard positioning and navigation. In: China satellite navigation conference (CSNC) 2012 proceedings. Lecture notes in electrical engineering, vol 159. Springer, pp 177–186. doi:10.1007/978-3-642-29187-6_17

Ge M, Zhang H, Jia X, Song S, Wickert J (2012) What is achievable with current COMPASS constellation? In: ION GNSS 2012

Gong H, Yang W, Wang Y, Zhu X, Wang F (2012) Comparison of short-term stability estimation methods of GNSS on-board clock. In: Sun J, Liu J, Yang Y, Fan S (eds) China satellite navigation conference (CSNC) 2012 proceedings. Lecture notes in electrical engineering, vol 160. Springer, pp 503–513. doi:10.1007/978-3-642-29175-3_46

Gurtner W, Estey L (2009) RINEX, the receiver independent exchange format, Version 3.01. Technical report. http://igscb.jpl.nasa.gov/igscb/data/format/rinex301.pdf

Han C, Yang Y, Cai Z (2011) BeiDou Navigation Satellite System and its time scales. Metrologia 48(4):S213–S218. doi:10.1088/0026-1394/48/4/S13

Hauschild A, Steigenberger P (2012) Combined GPS and GALILEO real-time clock estimation with DLRs RETICLE system. In: ION GNSS 2012

Hauschild A, Montenbruck O, Sleewaegen J, Huisman L, Teunissen P (2012a) Characterization of Compass M-1 signals. GPS Sol 16(1):117–126. doi:10.1007/s10291-011-0210-3

Hauschild A, Montenbruck O, Steigenberger P (2012b) Short-term analysis of GNSS clocks. GPS Sol. doi:10.1007/s10291-012-0278-4

Jun X, Jingang W, Hong M (2012) Analysis of Beidou Navigation Satellites in-orbit state. In: China satellite navigation conference (CSNC) 2012 proceedings. Lecture notes in electrical engineering, vol 161. Springer, pp 111–122. doi:10.1007/978-3-642-29193-7_10

Lyard F, Lefevre F, Letellier T, Francis O (2006) Modelling the global ocean tides: modern insights from FES2004. Ocean Dyn 56(5–6):394–415. doi:10.1007/s10236-006-0086-x

McCarthy DD, Petit G (2004) IERS conventions (2003) IERS technical note 32. Verlag des Bundesamtes für Kartographie und Geodäsie, Frankfurt am Main

Montenbruck O (2009) Orbital mechanics. In: Ley W, Wittmann K, Hallmann W (eds) Handbook of space technology. Wiley, West Sussex, UK, pp. 52–82. doi:10.1002/9780470742433

Montenbruck O, Hauschild A, Hessels U (2010) Characterization of GPS/GIOVE sensor stations in the CONGO network. GPS Sol 15(3):193–205. doi:10.1007/s10291-010-0182-8

Montenbruck O, Hauschild A, Steigenberger P, Hugentobler U, Teunissen P, Nakamura S (2012) Initial assessment of the COMPASS/BeiDou-2 Regional Navigation Satellite System. GPS Sol. doi:10.1007/s10291-012-0272-x

Niell A (1996) Global mapping functions for the atmosphere delay at radio wavelengths. J Geophys Res 101(B2):3227–3246

Pearlman M, Degnan J, Bosworth J (2002) The International Laser Ranging Service. Adv Space Res 30(2):125–143. doi:10.1016/S0273-1177(02)00277-6

Qian S, Jun Z, Yanbo Z (2012) China Compass PNT service architecture and outlook. In: ION ITM 2012, pp 848–854

Rebischung P, Griffiths J, Ray J, Schmid R, Collilieux X, Garayt B (2012) IGS08: the IGS realization of ITRF2008. GPS Sol 16(4):483–494. doi:10.1007/s10291-011-0248-2

Riley S (2012) Personal communication

Shi C, Zhao Q, Li M, Tang W, Hu Z, Lou Y, Zhang H, Niu X, Liu J (2012) Precise orbit determination of Beidou satellites with precise positioning. Sci China Earth Sci 55(7):1079–1086. doi:10.1007/s11430-012-4446-8

Shi C, Zhao Q, Hu Z, Liu J (2013) Precise relative positioning using real tracking data from COMPASS GEO and IGSO satellites. GPS Sol 17(1):103–119. doi:10.1007/s10291-012-0264-x

Soop E (1994) Handbook of geostationary orbits. Kluwer, Dordrecht. ISBN: 0-7923-3054-4

Steigenberger P, Hugentobler U, Montenbruck O, Hauschild A (2011) Precise orbit determination of GIOVE-B based on the CONGO network. J Geod 85(6):357–365. doi:10.1007/s00190-011-0443-5

Steigenberger P, Hauschild A, Montenbruck O, Rodriguez-Solano C, Hugentobler U (2012) Orbit and clock determination of QZS-1 based on the CONGO network. In: ION ITM 2012, pp 1265–1274

Svehla D, Heinze M, Rothacher M, Steigenberger P, Dähnn M, Kirchner M (2008) Combined processing of GIOVE-A and GPS measurements using zero- and double-differences. Geophysical Research Abstracts 10, sRef-ID: 1607–7962/gra/EGU2008-A-11383

Urschl C, Gurtner W, Hugentobler U, Schaer S, Beutler G (2005) Validation of GNSS orbits using SLR observations. Adv Space Res 36(3):412–417. doi:10.1016/j.asr.2005.03.021

Weber R (2012) IGS GNSS Working Group. In: Meindl M, Dach R, Jean Y (eds) International GNSS Service technical report 2011. Jet Propulsion Laboratory, Pasadena, pp 159–163

Weiguang G (2011a) ILRS SLR mission support request for Compass-G1. http://ilrs.gsfc.nasa.gov/docs/ilrsmsr_G11.pdf

Weiguang G (2011b) ILRS SLR mission support request for Compass-I3. http://ilrs.gsfc.nasa.gov/docs/ilrsmsr_I31.pdf

Withers DJ (1999) Radio spectrum management. Institution of Engineering and Technology

Wu JT, Wu SC, Hajj GA, Bertiger WI, Lichten SM (1993) Effects of antenna orientation on GPS carrier phase. Manuscr Geod 18:91–98